Electronic Supplementary Material (ESI) for New Journal of Chemistry.

Supporting information

The QM/MM-QTAIM approach reveals the nature of different reactivity of cephalosporins in the active site of L1 metallo-β-lactamase

Maria G. Khrenova,[*a,b] Alexandra V. Krivitskaya,[a,c] Vladimir G. Tsirelson[a,c]

[a] Federal Research Centre “Fundamentals of Biotechnology” of the Russian Academy of Sciences, Leninsky prospect, 33, bld. 2, Moscow, 119071 Russia

[b] Department of Chemistry, Lomonosov Moscow State University, Leninskie Gory, 1/3, Moscow, 119991, Russia

[c] Mendeleev University of Chemical Technology, Miusskaya Square, 9, Moscow, 125047, Russia

[*] E-mail: khrenova.maria@gmail.com

Section S1 Experimental data

Table SI-1. Rate constants k_{cat} obtained in the steady-state Michaelis-Menten conditions.

Compound	k_{cat}, s^{-1}	Reference
Cefoxitin 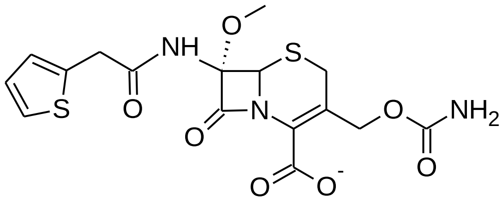	1.1	S1
Cefsulodin 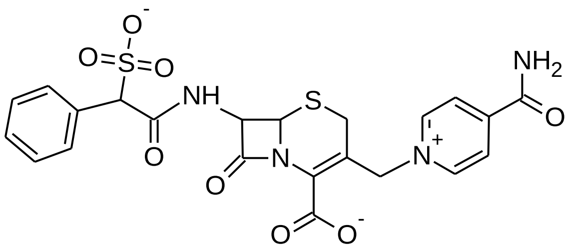	7.5	S1
CGP-17520A 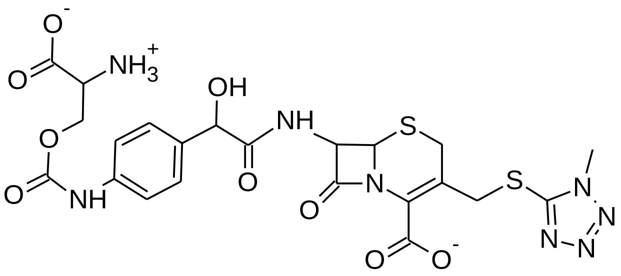	8.5	S1
Cefepime 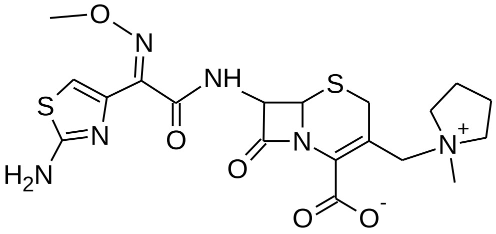	15	S2

Nitrocefin 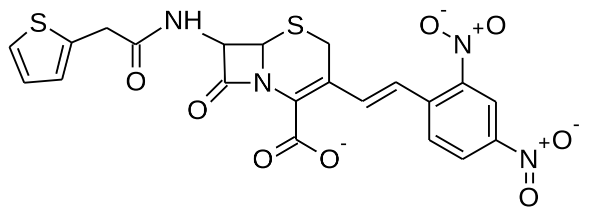	20	S1
Cephaloridine 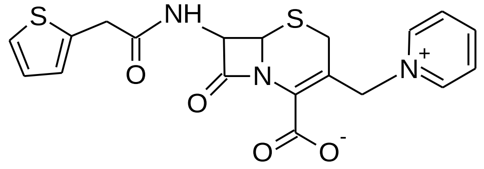	28	S2
CGP-31523A 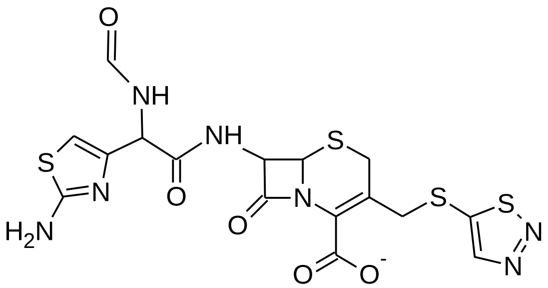	38	S1
Cephalosporin C 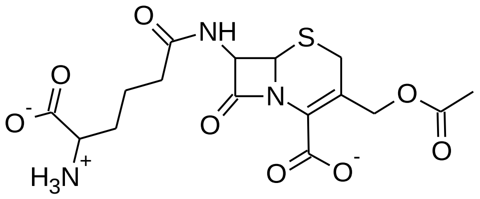	62	S2
Cefotaxime 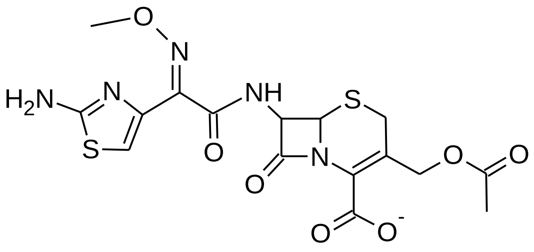	66	S2
Cefuroxime 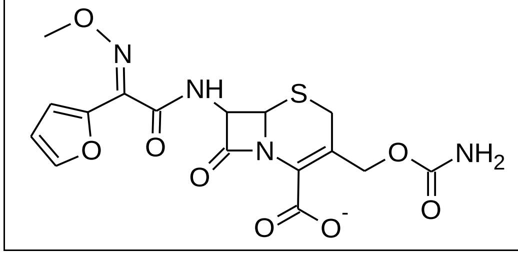	80	S2

Section S2 Atomic Charges

The atomic charges were calculated from atomic electron populations determined by the electron density integration the over the zero-flux QTAIM atomic basins. The charge on the oxygen atom of the aspartic acid becomes less negative upon O-H covalent bond cleavage during the limiting step. Contrary, the atomic charge becomes more negative on the O_s atom upon O_s-H bond formation in the transition state. Elongation of the coordination bond between N_s and Zn^{2+} during the limiting step results in the decrease of the absolute values of charges on both nitrogen atom and zinc cation. The charge on the transferring hydrogen atom becomes smaller upon formation of the transition state. Neither individual atomic charges at the stationary points nor their differences between the transition state and preceding intermediate demonstrate dependencies on the observed rate constants k_{cat}. Thus, these quantities cannot be utilized to quantify reactivity of the substrates.

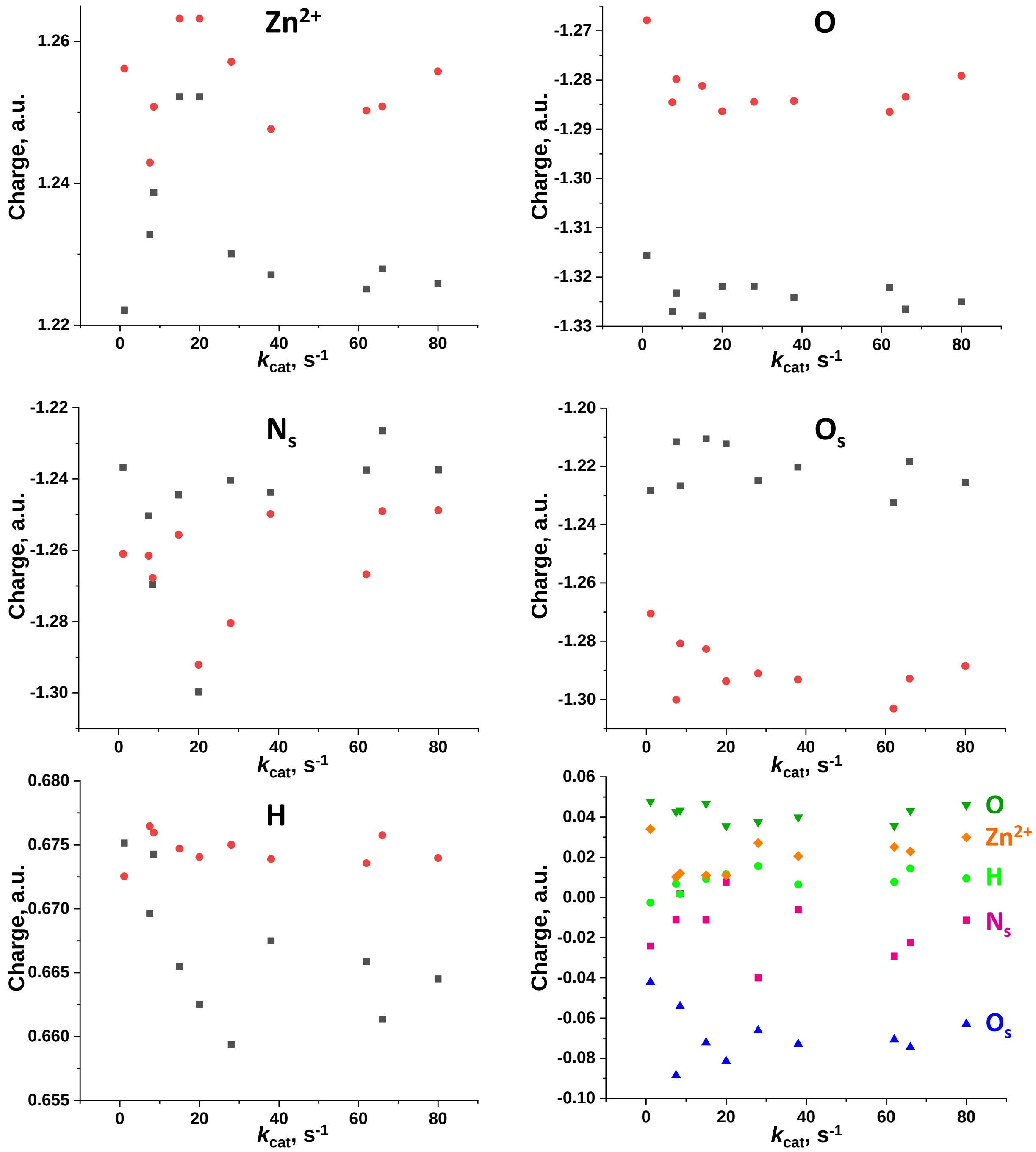

Figure S1. The QTAIM atomic charges in TS (grey squares) and Int (red circles) geometry configurations. The right bottom graph depicts the charge difference between the Int and TS stationary points of PES. The horizontal axis shows the experimental catalytic constants k_{cat} of the considered systems.

Section S3 Electron density based descriptors at Int and TS stationary points

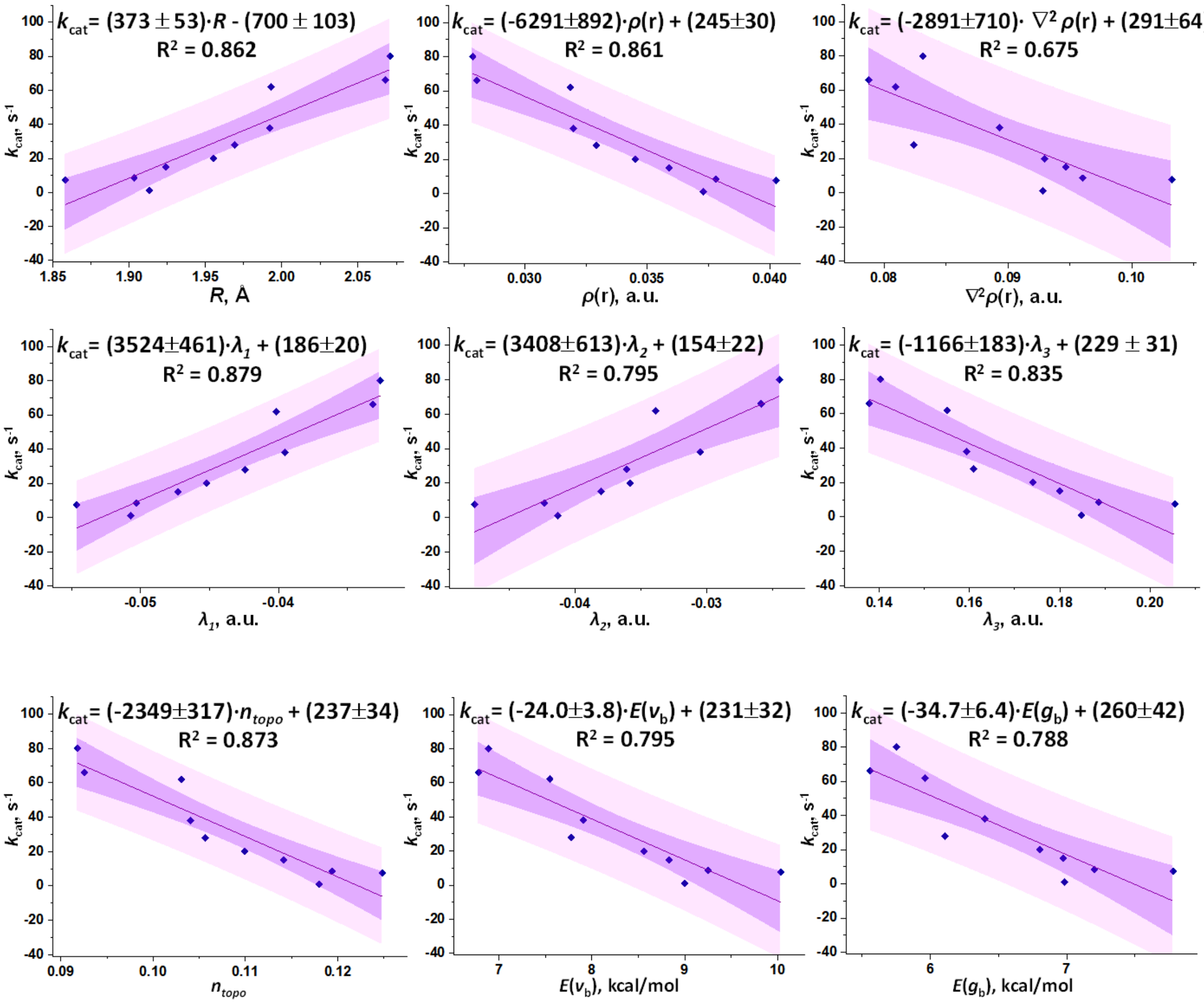

Figure S2. Descriptors of the N_S…H interactions at BCP-TS1 in TS geometry configuration *vs* experimental k_{cat} values. The dark red line demonstrates the linear trend, lilac and light lilac areas correspond to the 95% confidence and prediction bands, respectively.

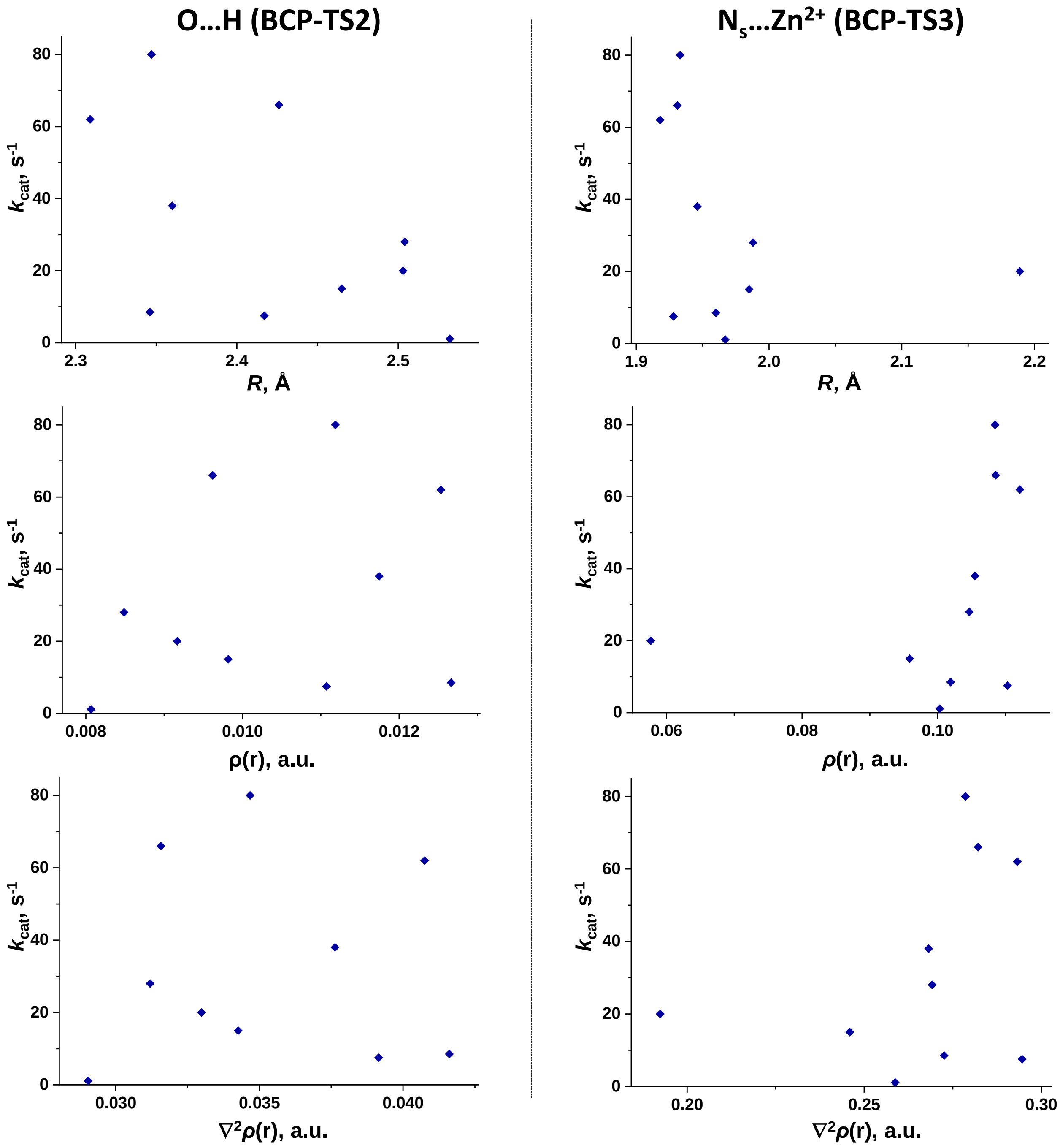

Figure S3. The interatomic distances, electron densities and Laplacians of electron densities calculated at BCP-TS2 and BCP-TS3 in TS geometry configurations plotted versus the experimental k_{cat} values of the respective model systems.

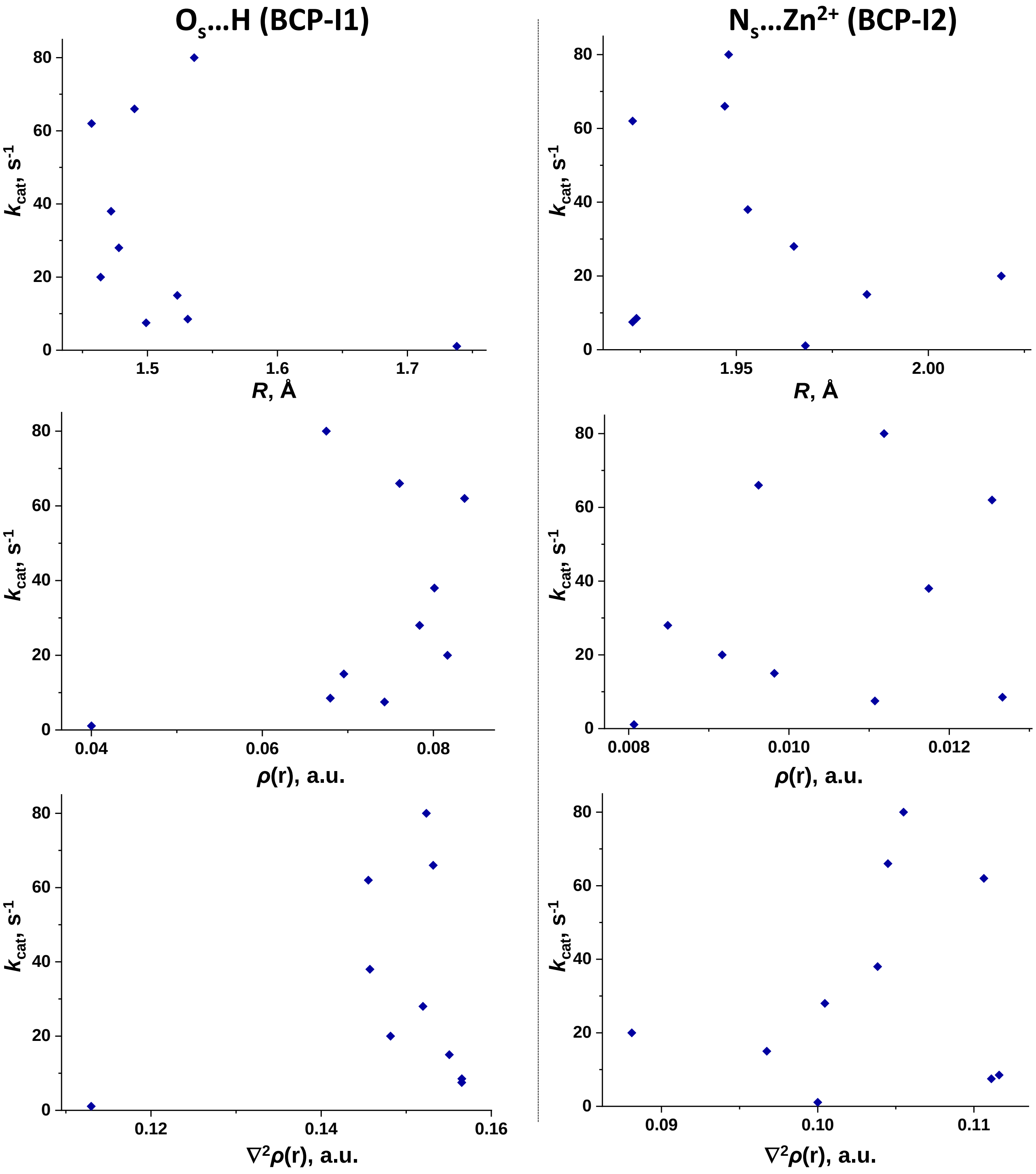

Figure S4. The interatomic distances, electron densities and Laplacians of electron densities calculated at BCP-I1 and BCP-I2 in the Int geometry configurations plotted versus the experimental k_{cat} values of the respective model systems.

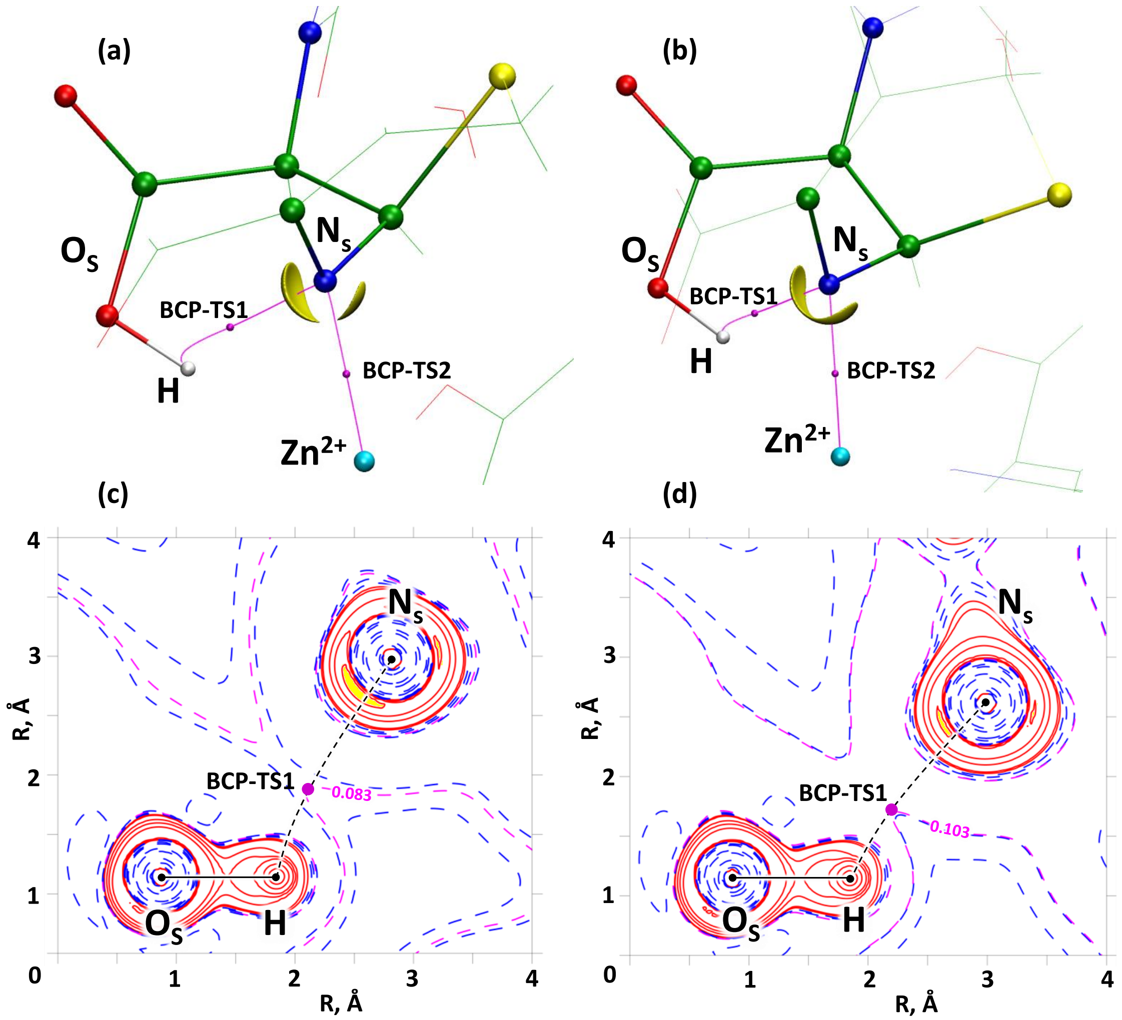

Figure S5. The Laplacian of electron density, $\nabla^2\rho(\mathbf{r})$, for the O_s-H...N_s fragment in the transition state geometry configurations of the MβL complexes with cefuroxime (a,c) or cefsulodin (b,d). The upper panel shows the 3D structure of the fragment of the active site and the $\nabla^2\rho(\mathbf{r})=-1.850$ isosurface. Bond critical points (BCPs) are magenta balls and bond paths connecting interacting atoms are shown in magenta dotted lines (a,b) or black dashed lines (c,d). Carbon, nitrogen, oxygen, hydrogen, sulfur and zinc atoms are colored in green, blue, red, white, yellow and light blue, respectively. The lower panels demonstrate cross sections of the surface formed by O_s, H and N_s atoms of the systems in upper panel. The contour lines correspond to the $\nabla^2\rho(\mathrm{r})$ values of $\pm(1;5)\cdot 10^n$, $-2\leq n\leq 2$. Positive contour lines (electron density depletion) are shown in dashed blue and negative ones (electron density concentration) are in solid red. Pink dashed contour lines denote the $\nabla^2\rho(\mathrm{r})$ values in BCP-TS1 of the corresponding systems: 0.083 for cefuroxime and 0.103 for cefsulodin. The areas of $\nabla^2\rho(\mathrm{r}) < -1.850$ inside the yellow region in upper panel is highlighted in yellow in lower panel. The values are given in a.u.

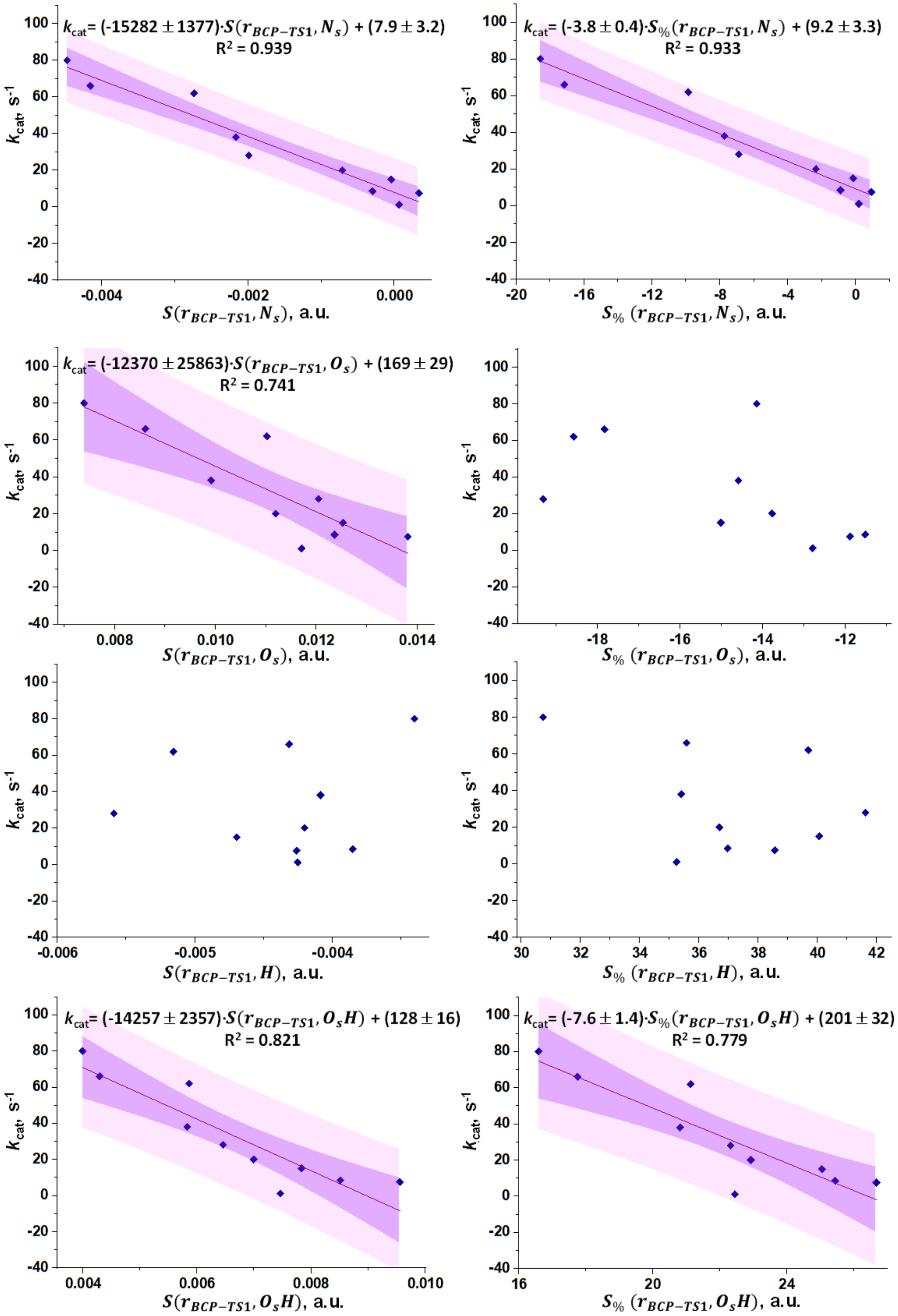

Figure S6. Dependences between the atomic contributions of electron density to BCP-TS1 and experimental k_{cat} values. The dark red line demonstrates the linear trend, lilac and light lilac areas correspond to the 95% confidence and prediction bands, respectively.

References

S1. Felici, A.; Amicosante, G. Kinetic Analysis of Extension of Substrate Specificity with Xanthomonas Maltophilia, Aeromonas Hydrophila, and Bacillus Cereus Metallo-Beta-Lactamases. *Antimicrob. Agents Chemother.* **1995**, *39* (1), 192–199.

S2. Crowder, M. W.; Walsh, T. R.; Banovic, L.; Pettit, M.; Spencer, J. Overexpression, Purification, and Characterization of the Cloned Metallo-β-Lactamase L1 from Stenotrophomonas Maltophilia. *Antimicrob. Agents Chemother.* **1998**, *42* (4), 921–926.